Traffic Analysis in Roundabout Intersections by Image Processing

L. Mussone*, M. Matteucci**, M. Bassani***, D. Rizzi**

* Politecnico di Milano, BEST, Milan, 20133, Italy
(Tel. +39 02 2399 5182; e-mail: mussone@polimi.it)
** Politecnico di Milano, DEI, Milan, 20133, Italy
(Tel. +39 02 2399 3470; e-mail: matteucci@elet.polimi.it)
***Politecnico di Torino, DITIC Torino, 10129, Italy
(Tel. +39 0115645635, e-mail: marco.bassani@polito.it)

Abstract: In this paper a method for the evaluation of roundabout performance, based on the image processing of field survey data, is presented. The methodology of investigation consists of the following three main steps: a field survey to collect vehicular flow images using video cameras, the processing of images gathered by the VeTRA (Vehicle Tracking for Roundabout Analysis) software program and the analysis of the trajectories extracted. The methodology enables the automatic computation of the information required to rank and evaluate a generic roundabout: the Entry/Exit (E/E) matrix with vehicle classification (i.e. heavy, light and motorbikes), identification of vehicle trajectories, and extraction of vehicular speed/curvature diagrams along the paths inside the roundabout. The proposed image processing stage overcomes classic problems encountered with image processing such as shadows, object occlusions, and the unpredictable influence of wind or clouds. Calibration and error evaluation are obtained from data collected by a high precision GPS-RTK system mounted on a probe vehicle.

1. INTRODUCTION

Nowadays, the roundabout is one of the most widely used solutions for road intersections, both in urban and rural environments and in European and other developed countries (Curti et al., 2008). This is mainly due to the potential benefits in terms of safer operations on the road network deriving from the reduction in operating speeds and in the number of conflict points with respect to traditional intersections. However, the performance of some roundabouts cannot be considered satisfactory and many of them could be improved in order to match driver expectations.

This lack of efficiency is normally attributed to less than optimum choices made at design stage, roundabout geometric dimensions and organization of elements (i.e., entry and exit lane width, central island diameter, entry and exit angles, angles between legs, etc.); all these factors affect functional performance in terms of capacity and safety. This has been confirmed by many studies (Rodegerdts et al., 2007) recently included in the Highway Safety Manual (TRB, 2010). The most interesting result relates to the fact that, under certain conditions, the conversion of a traditional intersection into a roundabout can lead to an increase in the number of accidents.

The aim of this paper is to introduce a survey methodology, developed to investigate such phenomena, which is based on the collection and analysis of video sequences. This methodology could be applied to the original intersection, prior to conversion into a roundabout, in order to gain the required knowledge regarding capacity requirement. It can then be applied to the new roundabout created to evaluate the effectiveness of same. As suggested also by Guido et al.

(2010), real trajectories and operating speeds, recorded directly from vehicles in a roundabout, can confirm whether the design assumptions are correct and how close to the expected performance the actual one is. In particular, expected performance can be verified by designers using swept path of turn, and comparisons can be carried out using speed and curvature diagrams. Moreover, it should be noted that operating speed diagrams can indicate whether the curvature of the four types of maneuvers (i.e., right-turn, crossing, left-turn and U-turn) leads to an effective speed reduction.

In the following, we present VeTRA (Vehicle Tracking for Roundabout Analysis), a software program developed to obtain true vehicle paths, kinematic variables, and the roundabout entry/exit (E/E) demand matrix through video analysis. It constitutes the first step in an extensive research, the purpose of which is to obtain efficient tools for the analysis of individual road elements. In the next section, pre-processing of images, vehicles tracking, and post-processing of data performed by VeTRA are described; in Section 3 the results obtained from the images collected in a field survey are presented (i.e. E/E matrix, flow classification, trajectories, and speed profiles); Section 4 provides some discussion of results, and outlines future research steps.

2. IMAGE PROCESSING IN VeTRA

2.1 Pre-Processing

For an accurate reconstruction of vehicle trajectories, a proper image pre-processing is needed on the images collected in the field survey as depicted in Figure 1. Firstly, the optical radial distortion, caused by less than ideal

camera lenses, has to be removed, so that lines and circles/ellipses in the scene correspond to lines and ellipses on the image plane. When doing this, the Bouguet camera model is computed by using calibration data, in the form of check-board images (Camera calibration toolbox, 2010) and is used for image un-distortion.

After un-distortion, image rectification is performed to recover constant pixel density of lines and angles for the projection of a specific plane of the observed world, i.e., the road pavement. This requires a homography between the pavement surface and the image plane to be recovered. In VeTRA we use a model based approach using the knowledge of the actual geometry of the intersection surveyed: the circular central island becomes an ellipse after perspective projection (Dihn et al. 2011).

In our case, a model of the external circle of the central island is built using (0,0) as central coordinates and the real radius of the central island. By applying the camera perspective transformation (partially known from calibration) to this geometrical model, the expected edge of the elliptical central island projection on the image plane is obtained. However, the true position of the camera with respect to the island (i.e. the extrinsic parameters) is unknown and needs to be estimated. In VeTRA, this is done by applying a genetic algorithm optimization procedure (Weise, 2009) in order to minimize the distance of the pixels in the real island contour of the image and the projection of the island model using camera calibration parameters, i.e., our unknowns. This optimization process provides a complete projective transformation from the 3D world to the 2D image and, by constraining world points to lie on the ground, this transformation becomes the homography we are interested in. A rectified image is then obtained having the roundabout in the center of the image and occupying the whole frame (see Figure 1).
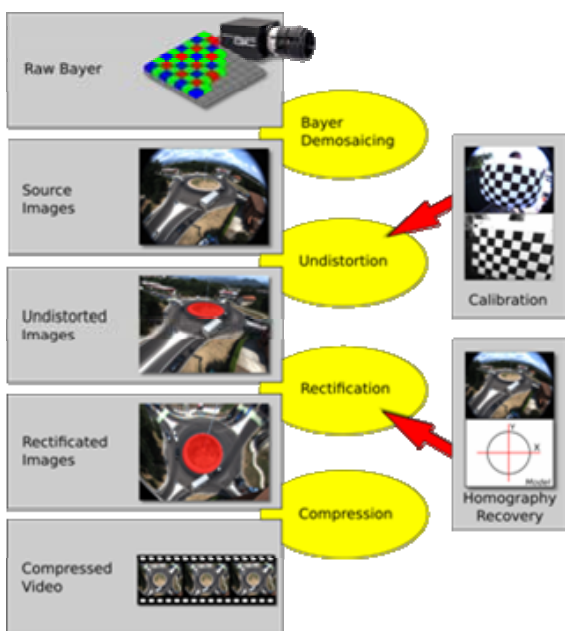

Fig. 1. The pre-processing chain of VeTRA software

2.1 Vehicle Tracking

Vehicle tracking in VeTRA is performed, on the movie resulting from pre-processing, by applying the following actions to each frame:

1. adaptive background modeling and subtraction to detect moving objects in the scene;

2. foreground identification through shadow and noise removal to get image areas representing vehicle (referred to as *blobs* hereafter);

3. association of newly detected blobs with previously tracked vehicles;

4. trajectory update for the tracked vehicles according to the new information.

All these activities rely on a proper model of the background that has to be robust with respect to changeable light conditions and camera displacements. In VeTRA this is achieved by the adaptation mechanism already introduced by Bonarini et al. (2006), in which each pixel is updated in the model by using a convex combination between its present value and the observed image. This updating mechanism is continuously performed in the areas of the image where no vehicles are present. A more detailed description of the background modeling approach can be found in the aforementioned paper.

Once the background model is available, vehicles can be extracted from the background by simple background subtraction, i.e. subtraction of the background model from the current frame. Pixels differing from the background beyond a given threshold (different for each pixel and derived from an estimate of the image noise for that pixel) are considered to be vehicles. In general, the above mentioned process overestimates vehicle size due to the presence of shadows. Since shadows affect the intensity of pixels, but not their hue and saturation components, VeTRA can establish whether a pixel belongs to the vehicle shadow or to the vehicle itself by using a threshold on the intensity channel. Morphological operators are then applied to the binary mask obtained at this stage in order to improve its quality by removing "salt and pepper" noise and filling gaps introduced by shadow removal.

Each vehicle in the scene is tracked across the sequence of images by using a Kalman filter (Grewal and Andrews, 2001) applied to blobs extracted in the image plane. In this context, the Kalman filter provides the a-posteriori probability of a vehicle position in the current image through the integration of a sequence of vehicle silhouettes extracted by the image processing algorithm. Kalman filtering requires a linear motion and a linear measurement models both affected by Gaussian noise; if such models are not linear it is possible to use the extended, i.e. linearized, version of the filter.

In VeTRA, the motion model f employed for the tracking of vehicles is a uniform circular motion and is expressed in a polar reference frame. The measurement equation h is given by the coordinates, in pixels, of the vehicle center on the image plane. The system state of the *k-th* vehicle

Kalman tracker comprises vehicle position (ρ, θ), radial and angular speeds (v, w), and the center of rotation (cx, cy), i.e. the center of the roundabout, in image coordinates:

$$f : \begin{cases} \rho_k = \rho_{k-1} + (v_{k-1} + \epsilon_{v_{k-1}}) \\ \theta_k = \theta_{k-1} + (\omega_{k-1} + \epsilon_{\omega_{k-1}}) \\ v_k = v_{k-1} + \epsilon_{v_{k-1}} \\ \omega_k = \omega_{k-1} + \epsilon_{\omega_{k-1}} \\ cx_k = cx_{k-1} + \epsilon_{cx_{k-1}} \\ cy_k = cy_{k-1} + \epsilon_{cy_{k-1}} \end{cases} \tag{1}$$

$$h : \begin{cases} x_k = \rho_k \cos(\theta_k) + cx_k + \epsilon_{mx_k} \\ y_k = \rho_k \sin(\theta_k) + cy_k + \epsilon_{my_k} \end{cases} .$$

State and measurements are assumed to be affected by uncorrelated, zero mean, Gaussian noise:

$$\begin{aligned} \epsilon_x &= [\epsilon_v, \epsilon_\omega, \epsilon_{cx}, \epsilon_{cy}]^T & \epsilon_{x_k} &\sim \mathcal{N}(0, R_k) \\ \epsilon_z &= [\epsilon_{mx}, \epsilon_{my}]^T & \epsilon_{z_k} &\sim \mathcal{N}(0, Q_k) . \end{aligned} \tag{2}$$

By expressing the motion in a polar reference frame, the equation involved can be simplified obtaining a linear Kalman update. From simulated runs and tests on real data, the use of polar coordinates offers better performances with respect to the same motion model expressed in a Cartesian reference frame. This can be understood by looking at the uncertainty representation, for a point in circular motion, given by this parameterization. Gaussian uncertainties in the (ρ, θ) motion plane translate into *crescent-shaped* uncertainties in the corresponding Cartesian frame (see Figure 2). This is sounder than the ellipse shaped error that we would otherwise obtain using a Cartesian reference frame, and it partially overcomes the limitations implied in the linear/Gaussian assumptions of Kalman Filter.

The outcome of the Kalman filter is an estimate of vehicle position with its uncertainty in the form of Gaussian distribution. This uncertainty information can be used to compute the Mahalanobis distance between the expected position of the tracked vehicle and its measured position when performing data association. The Mahalanobis distance is calculated between the blob center and the position predicted by the Kalman Filter (part of the state vector $\hat{x}_k^-$) with its associated uncertainty ($\hat{P}_k^-$). Being the position modeled in a polar reference frame, the blob center coordinates on the image plane $[m_{x_b}, m_{y_b}]^T$ are first converted to this frame:

$$d : \begin{cases} |(\rho_k + \epsilon_{\rho_k}) - \sqrt{\tilde{x}^2 + \tilde{x}^2}| \\ (\theta_k + \epsilon_{\theta_k}) - \mathrm{atan2}(\tilde{y}, \tilde{x}) \end{cases} \tag{3}$$

being

$$\begin{aligned} \tilde{x} &= (m_{x_k} + \epsilon_{mx_k}) - (c_{x_k} + \epsilon_{cx_k}) \\ \tilde{y} &= (m_{y_k} + \epsilon_{my_k}) - (c_{y_k} + \epsilon_{cy_k}) \end{aligned} \tag{4}$$

then the Mahalanobis (d_m) distance is computed as

$$d_m(m_k, \hat{x}_k^-) = \sqrt{d(m_k, \hat{x}_k^-)^T \Sigma_k^{-1} d(m_k, \hat{x}_k^-)} \tag{5}$$

and through uncertainty propagation we obtain the following formula for the filter covariance (being A_K and B_K the Jacobians of the Mahalonobis distance with respect
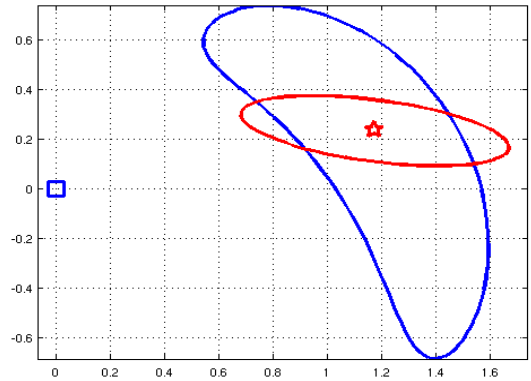

Fig. 2. Gaussian position uncertainty for a vehicle (the star) moving around the centre of the roundabout (the square) as represented, in the Cartesian plane, when using polar representation (dark grey) or Cartesian representation of the motion (light grey).

to errors):

$$A_k = \left.\frac{\partial d(m_k, x_k, 0, \bar{\epsilon}_x)}{\partial \bar{\epsilon}_x}\right|_{\bar{\epsilon}_x = 0} \quad B_k = \left.\frac{\partial d(m_k, x_k, \epsilon_z, 0)}{\partial \epsilon_z}\right|_{\epsilon_z = 0} \tag{6}$$

$$\Sigma_k = A_k \hat{P}_k^- A_k^T + B_k Q_k B_k^T$$

The evaluation of the difference in the center of mass of the blob and the tracked vehicle were chosen instead of the NIS (Normalized Innovation Squared), because, with the latter, the linearization carried on h wastes the physical meaning of the uncertainty of position estimate, by approximating the crescent shaped error with an ellipsoidal one (see again Figure 2). Blob to target Mahalanobis distance is not the only metric used to perform data association. In particular, the information about blob and tracker areas, perimeters and color histograms are used as well. For the scalar values (i.e., area and perimeter) a dissimilarity metric (d_s) is computed as the absolute value of the difference/sum ratio bounding it inside the (0,1) interval

$$d_s(a, b) = \left|\frac{a - b}{a + b}\right| \tag{7}$$

while, for histogram dissimilarity the (0,1) bounded Bhattacharyya distance (d_h) (Aherne et al., 1997) is used

$$d_h(H_a, H_b) = \sqrt{1 - \left(\frac{1}{\sqrt{\sum_j H_a(j) \sum_j H_b(j)}} \sum_i \sqrt{H_a(i) H_b(i)}\right)} \tag{8}$$

Blobs (identified with b hereafter) are then compared to targets (identified with t hereafter) by using a simple score that combines all these metrics:

$$\begin{aligned} score = &d_s(area_b, area_t) + d_s(perimeter_b, perimeter_t) + \\ &d_h(histogram_b, histogram_t) + d_m(centroid_b, EKFstate_t) \end{aligned} \tag{9}$$

The data association process is quite simple: all the blob-tracker pairs are evaluated, and for each pair the dissimilarity *score* is evaluated. A preliminary gating is performed, discarding blobs-tracker pairs that are too far

away (in a Euclidean sense) from each other. These pairs are assigned an infinite score. A second gating is carried out by looking at the score, discarding blob-tracker pairs whose score is greater than a given threshold; these pairs are also assigned an infinite score. Then all the scores are ranked in ascending order, and starting from the lowest score, blob-tracker pairs are associated. Multiple associations are prevented by tagging blob and tracker as already associated.

During Kalman filter updates, the area, perimeter, and histogram stored in the tracker are also updated using a first order low pass IIR filter (this technique is also called exponential smoothing). An adequate choice of the filter time constant implements the change in the size, or in the histogram of the tracked object, needed, for instance, in the presence of perspective deformations or variable light conditions.

On completion of the association procedure, the fate of the blobs and trackers depends on their association state: i) blobs that have no tracker associated become new trackers, and they are initialized with blob descriptors and a default TTL (Time To Live); ii) trackers that have an associated blob get updated using the information carried by the blob, and their TTL is reset to default value; iii) trackers that have no blob associated are allowed to live for TTL time steps evolving by Kalman filter prediction; iv) *dead* trackers are discarded, and trajectories, areas, and perimeters are logged.

2.2 Post Processing

From the trajectories obtained by the tracking algorithm the E/E matrix can be extracted. The E/E matrix represents the matrix of all flow movements in the roundabout and normally some differences between this and the corresponding matrix of other intersections are evident as the u-turn is possible in the case of the roundabout. To compute the E/E matrix from the computed trajectories, a specific algorithm has been developed. This is necessary since the tracking system is not capable of ensuring that all revealed trajectories are complete from entry to exit (due to variable factors such as noise, wind, shadows and clouds). Matrix reconstruction thus requires the following steps:

- deletion of trajectories with too short a length in terms of space and time (pure noise);
- separation of over-complex trajectories resulting from errors in blob detection and tracking;
- reduction of points in trajectories to avoid weird curves deriving from data association errors.

From the remaining data, the flow is computed by counting the number of intersections between trajectories and segments corresponding to the entry/exit lines. By adopting this solution all possible trajectories entering or exiting the circulatory roadway are considered and problems due to perspective deformations are avoided.

Trajectories on pavement surface can also be reconstructed from trajectories on the image plane and these can be obtained by using the known homography between the two planes. Although the homography used for image rectification could be re-used for this purpose, a different one has been used so as to increase the overall precision of the system. RTK-GPS data from an instrumented vehicle have been collected in synchrony with the image acquisition and a homography has been obtained between these data and the trajectory of the instrumented vehicle tracked by the VeTRA algorithm. To avoid outliers due to noise or other problems which lead to difficulties in the extraction of the homography between the RTK-GPS data and the image trajectories, the RANSAC method introduced by Fischler and Bolles (1981) was applied in the version proposed by Zuliani (2010).

By using the homography from an instrumented vehicle, it is possible to compensate for errors resulting from the difference between the center of mass of the blob associated with a vehicle and the projection of the center of mass of the vehicle. This requires different homographies for each vehicular class since they suffer significantly different deformations on the image plane. Classification of flow is also necessary to improve the overall performance of the flow count, speed diagram and trajectory path. A classification has thus been carried out to detect three classes of vehicle:

- bikes and motorbikes;
- light vehicles, vans and campers;
- heavy vehicles.

Classification consists of a local classifier and a voting system. The local classifier, implemented through a feed forward neural network, determines, for each frame, the vehicle class according to the position and area of the blob within the image.

Position is necessary since the same vehicle has different areas in different points of the image due to perspective deformation. The voting system collects the results of local classifiers for all points in the trajectory and then it selects the most frequent among the three different vehicle classes.

3. RESULTS

The results presented here are based on a survey carried out at a four-leg roundabout, located in a typical Italian urban environment (see Figure 3). The external diameter of the roundabout is 48 m and the circulatory roadway width is 11.6 m. The average width of entry links is 8 m with two lanes, and 6 m for exit ones.

As previously mentioned, the instrumentation used to collect the data for roundabout performance evaluation consists of a vision system and a RTK-GPS system both connected to a dedicated PC. The origin of the final reference system has been located in the center of the roundabout. It must be emphasized that, due to the particular position of the camera with respect to the center of the roundabout, the circulatory roadway between the legs 3 and 4 in Figure 3 presents the maximum occlusion effect.

TABLE 1. E/E matrix estimation (percentages refer to the total of crossing vehicles), and comparisons with values estimated manually by video analysis

VeTRA (1)					
Links	1	2	3	4	Tot.
1	0.483	3.384	22.149	0.514	26.531
2	3.267	0.234	4.930	7.966	16.397
3	19.229	3.411	0.000	7.510	30.151
4	1.896	11.599	13.201	0.226	26.922
Tot.	24.875	18.628	40.281	16.216	100.000
Average estimation of three operators (2)					
1	0.399	2.929	20.905	0.466	24.700
2	3.262	0.200	4.660	7.856	15.979
3	19.774	4.727	0.266	7.124	31.891
4	2.064	11.917	13.116	0.333	27.430
Tot.	25.499	19.774	38.948	15.779	100.000
Error (Difference 1-2)					
1	0.083	0.455	1.244	0.048	1.830
2	0.005	0.034	0.269	0.110	0.418
3	-0.544	-1.316	-0.266	0.387	-1.740
4	-0.168	-0.319	0.086	-0.107	-0.508
Tot.	-0.624	-1.416	1.333	0.438	0.000

3.1 E/E analysis

According to the methodology described above, the software detected 2,214 trajectories in the recorded video; 1,152 of which, their origin or destination not yet identified, were not directly associated to an E/E pair. The E/E matrix has been corrected by a two-step process:
  - an a-priori probability was calculated by valid trajectories (those with two intersection points);
  - unassigned trajectories were assigned to the matrix according this a priori probability.

This approach has been validated by a detailed check of all cases with one intersection point, where limited performance was due exclusively to occlusions.

By manual measurement, carried out by three operators on the same video recording, it was possible to evaluate the performance of the system. The data reported in Table 1 are the percentage of the total movements recorded by VeTRA and those derived by the three operators. In the last section of the table, the percentage difference between the two estimates confirms that there is an acceptable maximum divergence of 1.5%. It should be noted that this result is affected by the position of the camera and it could be improved further by a proper positioning of same. In fact, the trajectories coming from entrances 3 and 4, and those directed to the exits 1 and 2 are underestimated, since they cross the zone affected by occlusion effects (see Figure 3).

3.2 Flow classification

The local classifier can correctly classify about 98% of blobs in the trajectories. No ambiguity arises for heavy vehicles, but the distinction between some small vehicles and motorcycles appears to be less reliable. The voting schema has then been to group vehicles in all cases.
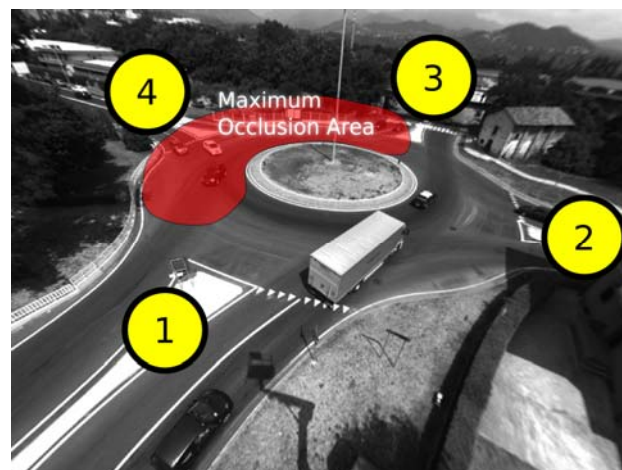

Fig. 3. Image of the roundabout considered for VeTRA validation

3.3 Trajectories and speed profiles analysis

Vehicle positions derived from the image analysis were compared with the corresponding positions derived from the RTK-GPS. The greatest distance between corresponding points is mainly evident on the legs. When a restricted analysis on the circulatory roadway is performed, distances between corresponding points are smaller. This leads to the conclusion that, for measurements regarding this case study, data on links need a better acquisition and must be excluded for software validation purposes.

The analysis of these data demonstrates the reliability of VeTRA:

  - median of position error is equal to 0.375 m;
  - median of absolute deviations (MAD) is 0.179 m;
  - inter-quartile range (IQR) is 0.399 m.

The comparison between speed values derived by VeTRA and those determined by the RTK-GPS has been considered taking the GPS data as reference. The error rate of VeTRA has a mean equal to 0.11 km/h and a standard deviation equal to 2.71 km/h. Those data have been calculated on 2.8 km traveled by the probe vehicle inside the circulatory roadway.

Figure 4A shows the curvature diagrams along the trajectory for one couple of E/E. In the diagrams, positive and negative values are considered according to the usual sign rule (positive for right turns and negative for left ones). Curvature lines are in grey, entry and exit sections are identified by black points while the average curvature line is black. Data are reported along the trajectory inside the roundabout referring to its middle point (0 m).

Speed profiles have been derived taking into consideration only those cars entering into the roundabout at a speed of not lower than 5 km/h, as, when operating speeds have to be derived, only isolated and unconditioned cars need to be considered. The 85th percentile of a sample of unconditioned speeds is commonly accepted as a good estimate of operating speed in a specific location.
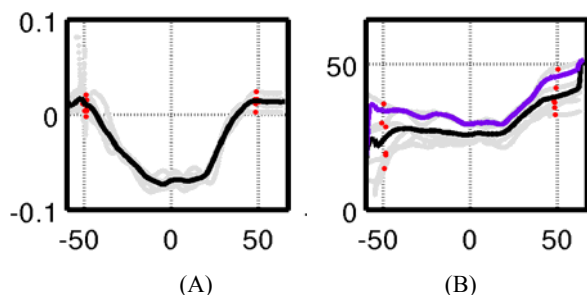
Fig. 4. (A) Curvature (grey curves) and average curvature (black curves) [1/m] profiles of the trajectories worked out for one E/E couple; (B) Speed profiles (light grey) [km/h] for the same E/E couple. Average speed (black curves) and operating speed (grey curves) diagrams. Initial and final points of trajectories in the circulating roadway are plotted as black points. X-axis in [m]

Figure 4B shows the speed profiles of each vehicle (light grey curves), the entry and exit points in the circulating roadway (red points), the average speed (black curve) and the 85th percentile speed (grey curve). Average and operating speeds are affected by moderate noise due to tracking system noise. It can be observed that operating speeds in the circulatory roadway are lower than 40 km/h.

4. CONCLUSION

In this paper a method for the analysis of roundabout performance, based on image processing, has been presented basing on a specific software program (VeTRA)

Results have proven that the software is very efficient in the evaluation of the E/E flow matrix, trajectories and speed profiles. Flow analyses performed by VeTRA have confirmed its capability of dealing with errors caused by occlusions. Comparisons with data derived by manual counting show a very low absolute average error of 0.7%, with a peak value of 2.1% while vehicle classification is reliable in all cases.

The trajectory reconstruction provides good results when the analysis is restricted to points close to the camera. Speed profiles are almost insensitive to tracking system errors. However, in a few cases, outliers and noise limit the performance of VeTRA and a smoothing algorithm is necessary to ensure more stable and reliable results.

The above mentioned performances encourage further VeTRA improvements including:
a) an image stabilization system to eliminate the effects of camera oscillations due to wind;
b) an improved background modeling and foreground extraction system for optimization in the presence of clouds, poor light and reflections;
c) an algorithm for the division and fusion of blobs to limit the effects of dynamic occlusions;
d) a simulation system in which vehicles are substituted by a 3D model in order to recover a precise relation

between the real position of cars and their position on the image plane without the need of the probe vehicle

A few of these improvements (a and b) have already been developed and integrated (though not yet tested) into the software. Moreover, the authors are working on new surveying approaches with respect to the camera arrangement. At this time, the following two options are being considered: vertical position in the center of the central island and lateral/central position of three cameras operating simultaneously. In both cases, the aim is the maximum possible reduction in the number of errors related to occlusion and perspective deformation.

REFERENCES

Aherne, F., N. Thacker, P. Rockett (1997). The Bhattacharyya metric as an absolute similarity measure for frequency coded data. Kybernetika, 32(4), 1–7.

Bonarini, A., D.A. Migliore, M. Matteucci, M. Naccari (2006). A revaluation of frame difference in fast and robust motion detection. Proc. of the 4th ACM International Workshop on Video Surveillance and Sensor Networks, pp. 215 - 218, New York, NY, USA.

Camera Calibration Toolbox, http://www.vision.caltech.edu/bouguetj/calib_doc/. Accessed Jul. 18, 2010.

Curti, V., L. Marescotti, L. Mussone (2008). *Roundabouts. Design and evaluations of roundabout intersections*. 4th ed., Maggioli S.p.A, Italy.

Grewal, M.S., A.P. Andrews (2001). *Kalman Filtering: Theory and Practice Using MATLAB*. John Wiley & Sons, Inc., New York, 2nd ed.

Guido, G. P., Saccomanno, F. F., Astarita, V., Vitale, A. (2009). Measuring Safety Performance at Roundabouts Using Videotaped Vehicle Tracking Data. Presented at 88th Transportation Research Board Annual Meeting.

Hai Dinh, Hua Tang, Eil Kwon (2011). Camera Calibration for Roundabout in Traffic Scenes. Presented at 90th Annual Meeting of the Transportation Research Board.

Rodegerdts, L., M. Blogg, E. Wemple, E. Myers, M. Kyte, M. Dixon, G. List, A. Flannery, R. Troutbeck, E. Brilon, N. Wu, B. Persaud, C. Lyon, D. Harkey, D. Carter (2007). *Roundabouts in the United States*. NCHRP Report 572, TRB, National Research Council.

TRB (2010). *Highway Safety Manual*. Transportation Research Board, National Research Council, Washington, DC.

Weise, T., Global Optimization Algorithms -Theory and Application 2nd Edition, Online as e-book, 2009.

Zuliani, M. *RANSAC Toolbox*. http://vision.ece.ucsb.edu/~zuliani/Code/Code.html, (2009). Accessed Jul. 18, 2010